

# ESTIMATING CLOUD ABSORPTION WITH TRMM/ PR, TMI RAIN-RATES, VIRS CLOUD RETRIEVALS AND CERES BROADBAND MEASUREMENTS

Y.-X. Hu, B. Wielicki and Q. Fu  
MS 420  
NASA Langley Research Center

## 1. Introduction

Solar radiation measurements suggest that clouds absorb more solar radiation than most GCM model calculations. There has been considerable debate on the magnitude of the discrepancy between observations and model calculations.

Here we seek to find cloud targets for which the absorption can be accurately estimated from satellite measurements, and compare the measurements with comprehensive radiative transfer model calculations. The targets in this study are extensive deep convective cloud systems with large cloud water path (i.e., those clouds with heavy rainfall) and very low cloud top temperatures. By building accurate anisotropy models suitable for such these cloud systems, we can accurately measure the TOA albedos of these clouds. **Because the transmissivities for these optically thick clouds are almost negligible, their absorption can be accurately estimated from CERES measurements.** The specific goals of this study are to:

- **build adequate anisotropy models** for deep convective cloud systems from Clouds and the Earth's Radiant Energy System (CERES) observations. With the new anisotropy models, we will be able to **get unbiased albedos from CERES measured shortwave radiances**;
- **identify the extensive deep convective clouds with large water path from narrowband measurements and accurately evaluate their albedos from CERES measurements**;
- accurately **compute broadband fluxes and radiances** with cloud property retrievals from narrowband observations **to compare with the broadband measurements.**

## 2. DATA AND MODELS

### TRMM/CERES, VIRS, Precipitation Radar and Microwave Imager

0

The radiance data from TRMM / CERES ERBE-like Instantaneous TOA radiances (ES8) between Jan. 1 and Aug. 31 of 1999 have been analysed to build an initial set of anisotropy models for deep convective clouds. The radiances from the CERES single satellite footprint (SSF) product, for which the geolocation is referenced to the surface, together with collocated cloud optical properties retrieved from the Visible Infrared Scanner (VIRS) (Minnis, et al., 1998), will be used for albedo inversion. The CERES radiances include broadband shortwave, longwave window and longwave total, filtered as well as unfiltered. The VIRS data in the SSF includes CERES footprint-averaged (both linearly and logarithmically) cloud optical depth and effective particle size retrieved from visible and near-IR channels. The variances of the VIRS imager-level cloud temperature and within the footprint will be studied in order to eliminate the CERES footprints which are horizontally heterogeneous. The combined rain rate profiles (TRMM data 2B-31) from TRMM precipitation radar (PR) and 10 GHZ channel of TRMM microwave imager (TMI) will be collocated with CERES footprint broadband radiance data. With the help of the rain rates, we will

be able to single out the optically thick deep convective cloud systems with very small vertical transmissivity.

### Deep Convective Cloud Anisotropy, $\text{sza}=41^\circ$

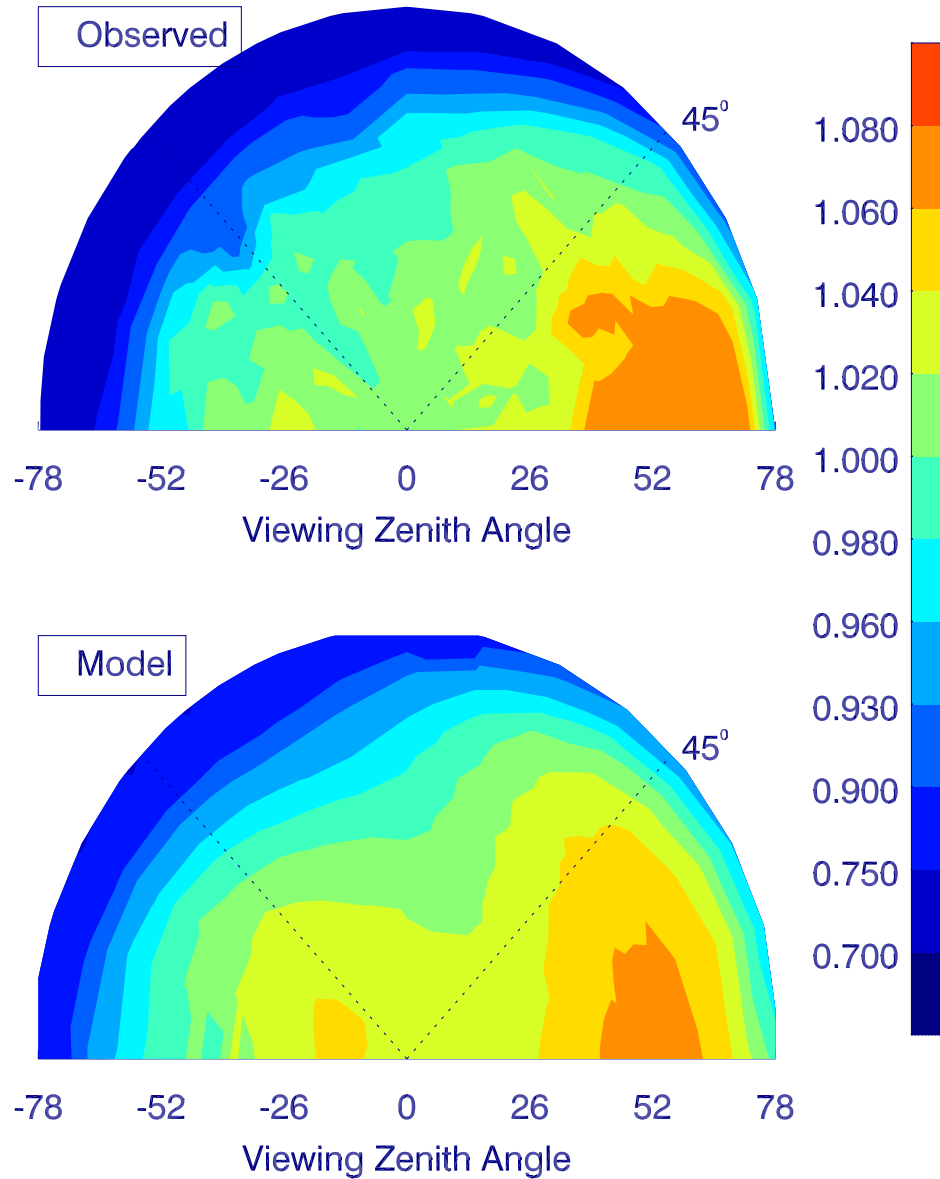


**Figure 1:** Anisotropy factors from CERES observations (upper panel) and from DISORT model calculations (lower panel) for clouds colder than 205K. Solar zenith angle: 38 - 41 degree.

#### Radiative Transfer Model

0

The discrete ordinates radiative transfer (DISORT) model [Stamnes, 1988] is used to account

for cloud multiple scattering. On average, at close nadir view a photon has to bounce more than 10 times before it leaves deep convective clouds and reaches the sensor. Proper treatment of the phase function, especially the forward peak, becomes very important. A fast and accurate treatment of the phase function (Hu *et al.*, 1999) is adopted in order to compute the radiances accurately with less than 40 streams. With this model, the whole shortwave spectrum (0.3–4  $\mu\text{m}$ ) is divided into 24 bands with about 10 different absorption values in each band. The absorption from  $\text{H}_2\text{O}$ ,  $\text{O}_3$ ,  $\text{O}_2$ ,  $\text{N}_2\text{O}$  and  $\text{CH}_4$  is included. Special treatment of Rayleigh scattering in the UV and visible bands are adopted in order to choose the best weights for the Rayleigh scattering optical depth of each band. Cirrus optical properties of 24 different wavelength bands are derived for a set of 7 ice crystal size distributions based on *in situ* measurements of cirrus. The cirrus distributions are composed of a combination of hexagonal plates, hollow columns, bullet rosettes, and aggregates. Yang *et al.* (1997) provide a detailed explanation of the methods used to describe scattering calculations for hollow columns and bullet rosettes, and Yang and Liou (1998) describe calculations involving more complex crystals such as aggregates.

### 3. Results and Discussions

#### Deriving Anisotropy Models Suitable for Deep Convective Clouds

0

The key to improving the accuracy of observed albedos is to build accurate anisotropy models.

Anisotropy models ( $R$ ) are the observed relations between radiances ( $I$ ) and fluxes ( $F$ ) at every incident and viewing angles:  $R = \pi I/F$ . Both  $I$  and  $F$  for every scene type are statistically averaged values generated from months of observations. In general, the broadband anisotropy factors are much less sensitive to the optical depth and cloud heterogeneity, comparing with the radiance field. Such an insensitivity is one of the key factors of the concept we propose for obtaining accurate measurements of cloud absorption. The first step toward building an unbiased anisotropy model is to choose the criteria which characterize the similar clouds (scene identification). We collected radiances for clouds with CERES window temperature lower than 205K for all 8 months of CERES ES8 data. We then divide the data into 3375 angular bins (15 solar zenith, 15 viewing zenith and 15 relative azimuth). The relative azimuth bins are equal distance in angles ( $\Delta\phi$  is a constant). Solar and viewing zenith ( $\mu$ ) bins are divided into equal flux bins ( $\Delta\mu^2$  is a constant).

For each solar zenith angle bin, the radiances at every viewing angle bin are averaged with proper weights in order to derive the averaged fluxes. Then, we derive the anisotropy factors for all viewing angles with the solar zenith bin. These are simply the averaged radiances at each viewing zenith bin times  $\pi$  divided by the flux. The most dangerous errors in building the anisotropy models are putting one type of cloud in one viewing zenith bin and putting another type in others. It is more serious than putting thin and thick clouds together for every angle. Are we making this mistake when we use cloud temperature colder than 205K?

To check whether we are looking at the same group of clouds for all the viewing angles, we examined cloud optical depth distributions for different viewing angles when the clouds are colder than 205K. The optical depths are retrieved from VIRS (Minnis *et al.*, 1998). The retrieved results show that the retrieved optical depths for different viewing angles are very close. It implies that clouds colder than 205K are the same group of clouds even though we view them from different

angles. Cloud 3-D effects might have contributed slight differences at nadir view.

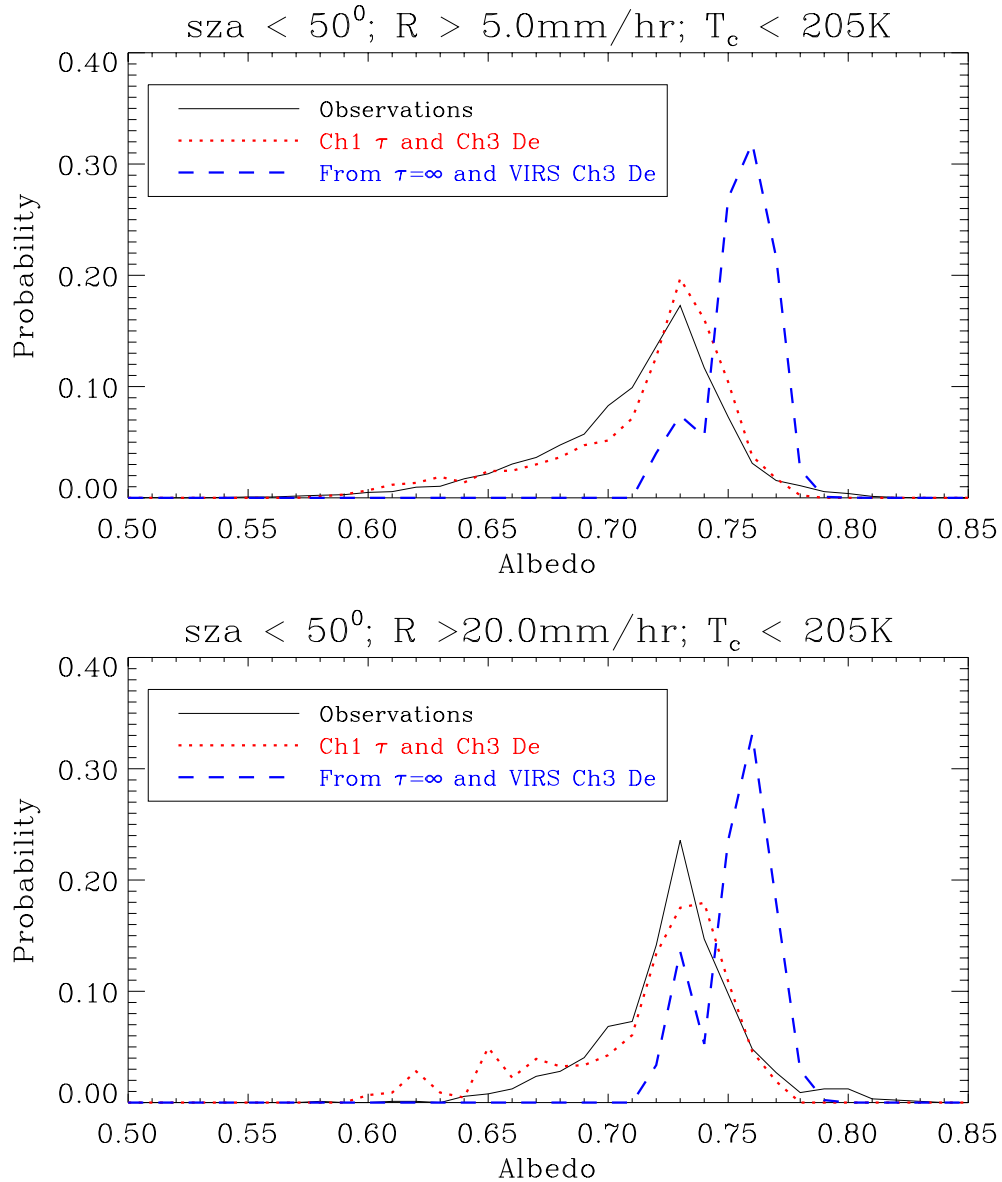


**Figure 2:** albedos from observations (solid curves), calculations with VIRS channel 1 optical depth (dotted curves) and calculations with very large optical depth (dashed curves).

#### Albedos of non-transparent deep convective clouds

0

- Identify non-transparent convective clouds: extensive cold clouds with large cloud water path  
The brightness temperatures of clouds with optical depths 5 and 1000 are not very different if the cloud top height is the same. So, cold clouds do not necessarily mean thick clouds. We cannot rely completely on cloud temperature to identify the thickest convective clouds. It is better not to

rely on visible channel to screen out thinner clouds, either, because we are looking for signals of anomalous absorption and we can not completely rule out the problem of visible absorption (Cess *et al.*, 1999). Using a visible channel to screen out thinner clouds will over-estimate reflection because the dark side of a heterogeneous cloud is considered as a thinner cloud and left out.

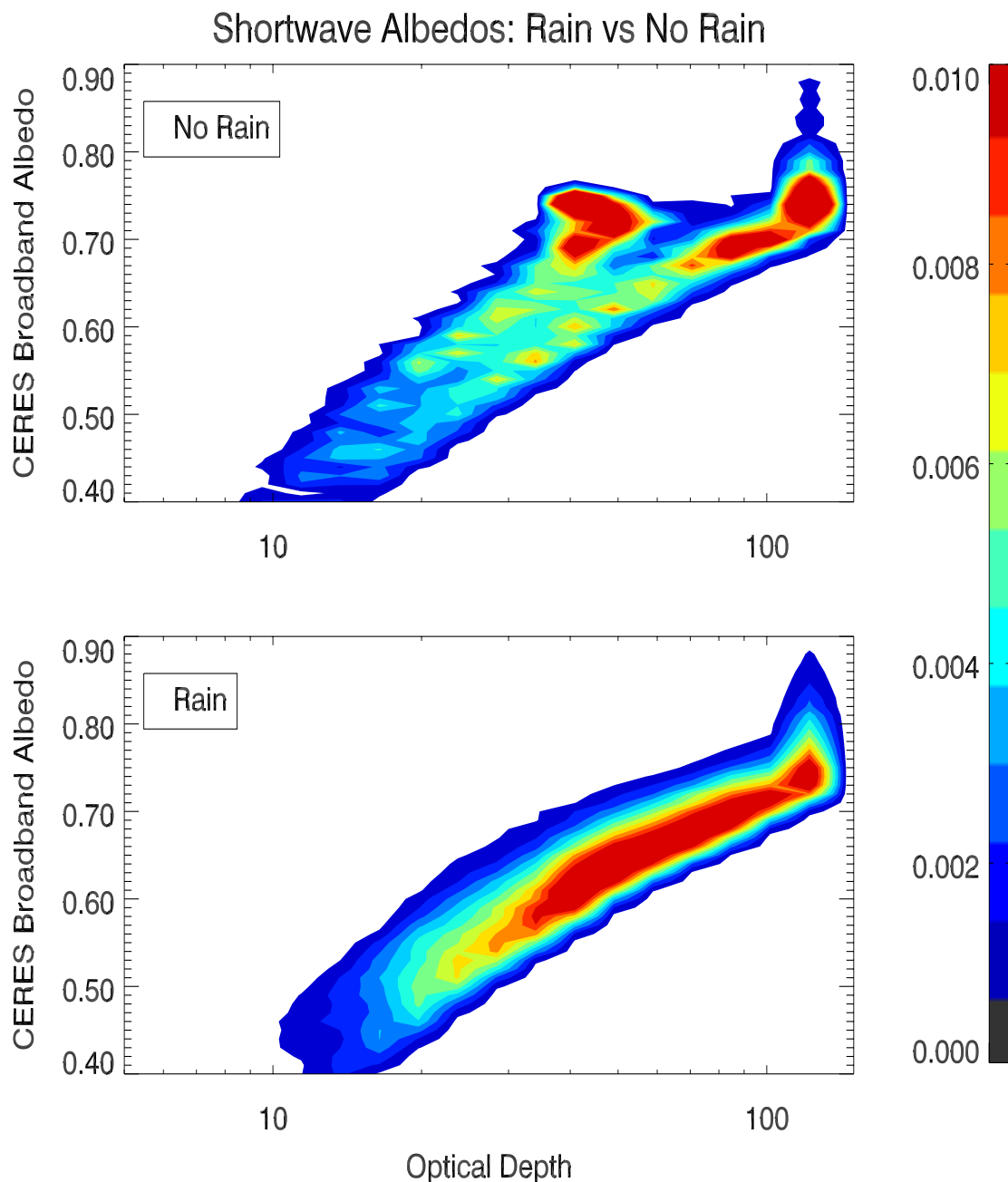


**Figure 3:** *Probability of observations available for different albedos and  $\tau$*

Non-transparent clouds have huge cloud water path. Cloud water path is positively correlated with rain rates (Lin, 1995). With the help of TRMM precipitation radar (PR) and 10 GHz micro-

wave imager (TMI) data, it is possible to identify heavily raining footprints. Common sense tells us that these footprints are almost completely opaque, although this assumption needs to be verified by surface observations. The 10 GHZ TMI data has a huge footprint and thus can be used to assure the horizontal homogeneity.

We collected the combined PR and TMI rain rate data from TRMM dataset 2B31 with collocated CERES broadband data in order to derive the average surface rain rate of each CERES footprint. The distribution of albedo for heavily raining, very cold, deep ( $T < 205\text{K}$ ) convective regions. The mode of the albedo is 0.73 (solid curves) for solar zenith angle less than 50 degree. The standard deviation of the albedo distribution for heavily raining footprints (rain rates larger than 20 mm per hour) is about 0.04. The standard deviation is contributed by cloud heterogeneity as well as the albedo - solar zenith angle dependence.

The averaged albedos increase with rain rates slightly because of the decrease in transmissivity. The mode of albedo increases from 0.72 to 0.73 when rain rate increases from 1 mm per hour to 20 mm per hour and then stays the same for larger rain rates.

- Comparison with model calculations of broadband albedo from VIRS optical property retrievals

With optical depths and effective particle sizes retrieved from TRMM/VIRS, we are able to compare computed broadband radiances and fluxes with CERES observations. The computed broadband fluxes with optical properties retrieved from VIRS (dotted curves) are close to CERES observed fluxes. The mode of optical depth for heavily raining (rain rate greater than 20 mm per hour) clouds with temperature less than 205K from VIRS retrievals is less than 70 and the averaged effective particle diameter is 80 micron. However, these retrieved optical depths are far less than what we would expect from microwave cloud ice and water path retrievals (Lin, 1995; Liu and Curry, 1999). The associated average transmissivities from calculations (more than 15 percent in visible and 7 percent total) are much larger than what we would expect. Narrowband calibration, the unknown absorption in the visible spectral region (Cess *et al.*, 1999) and vertical inhomogeneity might also contribute to the relatively low optical depths.

It is likely that the surface insolation for these clouds is very small, perhaps only one or two percent. Statistics from surface observations are needed to verify this suggestion. If surface observations support that these clouds are non-transparent and if 3-D effects are small, **the averaged absorptivity for these clouds will be around 27 percent.** The optical depths for these clouds will also be very large. As a result, the computed albedos will be about 3.5 percent higher than CERES observations. Large rain droplets,  $\text{NO}_2$  absorption associated with lightning (Solomon *et al.*, 1999) and vertical particle size variations may explain these differences.

### 3. SUMMARY:

The transmissivities of deep convective clouds with large liquid water paths are very small. The albedos of these nearly opaque, deep convective clouds can be accurately assessed from CERES measurements. Thus the absorption by those clouds can be accurately estimated. The fluxes and radiances of these clouds can also be computed from a comprehensive radiative transfer model with the help of narrowband cloud retrievals from visible and infrared channels. The measured albedos and their angular dependences are compared with model calculations.